Supplementary Information

Structural basis of G protein-coupled receptor/G protein interactions

Jianxin Hu, Yan Wang, Xiaohong Zhang, John R. Lloyd, Jianhua Li, Joel Karpiak, Stefano Costanzi, and Jürgen Wess

Supplementary Methods

Biotinylation of cell surface proteins and isolation of biotinylated M3R/Gα_q complexes. Cell surface proteins were biotinylated using a protocol similar to that described by Chen *et al*.[1]. About 48 h after transfection, COS-7 cells were washed twice with PBS. Cells were then incubated for 10 min (room temperature) with EZ-Link^{TM} sulfo-NHS-SS-biotin (1.5 mg in 1 ml of PBS; pH 8.0; Thermo Scientific). After this initial incubation step, a new aliquot of EZ-Link^{TM} sulfo-NHS-SS-biotin (1.5 mg in 1 ml of PBS; pH 8.0) was added, followed by another 10-min incubation at room temperature. The biotinylation solution was then removed, and 1 ml of 0.1 M glycine (in PBS; pH 8.0) was added to each 100-mm dish, followed by a 10-min incubation at 4 °C. Subsequently, 2 ml of ice-cold buffer A (25 mM sodium phosphate and 5 mM $MgCl_2$, pH 7.4) was added to each dish, followed by a 10-min incubation at 4 °C. Cells were then scraped off the plates, homogenized, and centrifuged as described under Methods (Preparation of membranes from transfected COS-7 cells). Membrane pellets were resuspended in 1 ml of ice-cold buffer A and homogenized as described above. Gα_q/M3R cross-linking studies were carried out using BMOE (0.5 mM) as a chemical cross-linker, followed by membrane lysis, as described under Methods (Disulfide cross-linking and solubilization of Cys-substituted Gα_q and M3R proteins). Subsequently, 30 µl of ImmunoPure® immobilized streptavidin (50% slurry, Thermo Scientific) was added to the samples, which were then incubated at 4 °C with end-over-end rotation (30 rpm) for 15-20 h. Samples were then centrifuged at 1,000 x *g* at 4 °C for 5 min, and the supernatants were discarded. The agarose pellets were washed with 0.1% digitonin in PBS (pH 7.4). This

centrifugation/wash step was repeated three times (the last wash step was carried out in the absence of digitonin). The agarose pellets were then incubated with Laemmli sample buffer containing 10% β-mercaptoethanol for 15 min at 37 °C (reducing conditions), followed by SDS-polyacrylamide gel electrophoresis (PAGE) and Western blotting using a monoclonal anti-$G\alpha_q$ antibody (see Methods for details).

Co-immunoprecipitation studies. Membrane samples from COS-7 cells co-expressing mutant M3R and $G\alpha_q$ proteins, either alone or in combination, were subjected to the cross-linking procedure described under Methods. Solubilized proteins (~600 μg) were then incubated for 1 hr at 4 °C with either the anti-$G\alpha_q$ monoclonal antibody directed against residues 22-31 of human $G\alpha_q$ (5 μg; BD Biosciences) or the rabbit anti-M3R polyclonal antibody (5 μg) directed against the C-terminal 18 amino acids of the rat M3R. Subsequently, 30 μl of protein A/G-agarose (anti-$G\alpha_q$ antibody) or protein A-agarose (anti-M3R antibody) were added, and the incubation was continued for an additional 1 hr at 4 °C. The protein A/G- or protein A-agarose was washed three times with 0.2% digitonin in PBS buffer, and bound immunoreactive proteins were then eluted at 37 °C for 15 min with 40 μl of 1 x Laemmli loading buffer either in the absence (to study cross-link formation for the N357C-$G\alpha_q$/T556C-M3R and R31C-$G\alpha_q$/L173C-M3R pairs) or the presence of 10% β-mercaptoethanol (to study cross-link formation for the D321C-$G\alpha_q$/K548C-M3R combination). Twenty μl of sample was loaded per lane, and immunoblotting studies were performed as described under Methods.

In-gel tryptic digestion of proteins. To authenticate the identity of the ~80 kDa immunoreactive band observed in the cross-linking studies, we carried out LC/MS/MS experiments to obtain partial sequence information. For these studies, the N357C-$G\alpha_q$/T556C-M3R pair was chosen as a representative $G\alpha_q$/M3R combination. Membranes were prepared from COS-7 cells co-expressing the N357C-$G\alpha_q$/T556C-M3R combination. Following membrane lysis, ~2 mg of solubilized membrane proteins were immunoprecipitated with 15 μg of the polyclonal anti-M3R antibody. Bound immunoreactive proteins were washed, eluted, and resolved by SDS-PAGE as described above. The ~80 kDa immunoreactive band predicted to represent a cross-linked

$G\alpha_q$/M3R complex (N357C-$G\alpha_q$/T556C-M3R) was excised from the protein gels with a scalpel. The gel section was transferred to a pre-washed 500 µl microfuge tube and divided into four sections with a scalpel. The gel pieces were washed two times with 200 µl of a 1:1 mixture of 100 mM ammonium bicarbonate (AMBIC) and acetonitrile (Sigma-Aldrich) for 45 min at 37 ºC. After the second wash, the supernatant was removed with a micropipette, and the gel pieces were dried in a SpeedVac (Savant). Reduction/alkylation was performed by addition of 100 µl of 2 mM TCEP (tris(2-carboxyethyl)phosphine) in 25 mM AMBIC to the dried gel, followed by a 30 min incubation period at 57 ºC with agitation. The supernatant was then removed, and 100 µl 0.55 M iodoacetamide (GE Healthcare) in 25 mM AMBIC was added. After a 30 min incubation in the dark at 37 ºC, the supernatant was discarded, and the gel pieces were washed three times with 200 µl of 25 mM AMBIC for 15 min. The supernatant was discarded, and the gel pieces were dried completely in a SpeedVac. Trypsin digestion was performed by rehydrating the gel pieces with 20 µl of 2 ng/µl of sequencing grade modified trypsin (Promega) in 10% acetonitrile, 50 mM AMBIC, and 0.01% ProteaseMax (Promega) surfactant for 30 min on ice, allowing the trypsin to diffuse into the dehydrated gel pieces. After removal of any remaining trypsin solution, 50 µl of 10% acetonitrile, 50 mM AMBIC and 0.01% surfactant were added. The sample was then incubated for 3 hr at 37º C. To stop the trypsin digestion, 50 µl of 2.5% trifluoroacetic acid (TFA; Sigma-Aldrich) was added to the gel pieces, and the supernatant was collected in a fresh tube. Subsequently, 50 µl of 2.5% TFA was added to the gel pieces and samples were incubated for 15 min at 37 ºC. The supernatant was removed and added to the previous collection tube. The collected supernatants were dried with a SpeedVac and resuspended in 200 µl 2.5% TFA. The sample was then dried again with a SpeedVac.

LC/MS/MS analysis. Twelve µl of 0.2% TFA solution were added to the dried tryptic digest. Ten µl of this solution were desalted/trapped on a 2 cm C8 capillary column (New Objective). The LC system was a CapLC pump (Waters) operated at 12 µl/min. LC flow was split using a backpressure regulator (Model p-880, Upchurch Scientific), resulting in a 200 nl/min flow through the analytical column (New Objective C18, 1.7 µm x 75 µm x 10 cm). Solvent A was an aqueous solution of 0.2% formic acid and 2% acetonitrile.

Solvent B was 2% water in acetonitrile with 0.2% formic acid. The tryptic peptides were eluted using a 40 min gradient from 0 to 60% of solvent B. MS/MS data were obtained using the LTQ mass spectrometer (Thermo) operated in data-dependent MS/MS mode. The top five MS ions were selected for MS/MS with a threshold of 1500 counts. Singly charged ions were excluded. The AGC settings for MS mode were 600 ms and 1 x 10^5 ions. The corresponding settings for MS/MS mode were 500 ms and 3 x 10^4 ions. The ESI nanospray tip was a coated version and had a 15 μm (internal diameter) spray orifice (New Objective). The ESI voltage was 2.2 kV. The scan range for MS mode was 475-1600 Da. To enhance the sensitivity of ion detection, a background ion reduction device (ESI Source Solutions) was used. The CID energy was 35 volts. The raw data file was converted to concatenated dta format with RawExtractor software (The Yates Lab, The Scripps Research Institute). The dta file was searched using the Mascot server (Matrix Sciences). Representative MS/MS spectra are shown in **Supplementary Fig. 6**.

Construction of M3R and G_q homology models. All homology modeling procedures were conducted with MOE (version 2008.10, Chemical Computing Group Inc., 2008) using the CHARMM22 force field. Before the procedure, the template was protonated with the Protonate3D function of MOE (ref. 2). Initial automatic sequence alignments were obtained with the Blosum62 substitution matrix, with penalties for gap insertions and extensions of 7 and 1, respectively. All the gaps in the alignment of regions with defined secondary structure were eliminated. Gaps in the unstructured loops were consolidated into a single gap per loop, and positioned where insertions or deletions seemed compatible with the structure of the template. The sequence alignments used for the construction of the receptor and G protein models are shown in **Supplementary Figs. 13** and **14**. For the receptor, the proper alignment of the conserved motifs that characterize each of the seven TM helices was also checked. For each target, ten models were built and scored on the basis of electrostatic solvation energy (GB/VI)[3]. Intermediate and final models were subjected to energy minimizations with the CHARMM22 force field, until reaching a cutoff parameter on the potential energy gradient of 1 kcal/(mol Å) for the former and 0.5 kcal/(mol Å) for the latter. The homology model of the rat M3R (residues 65-205, 220-261 and 484-560) was

constructed on the basis of the structure of the turkey β_1-adrenergic receptor in complex with cyanopindolol (2VT4)[4]. The two receptors show 33.5% sequence identity (at the amino acid level) in the modeled regions. Notably, this level of sequence identity is generally considered sufficient to generate accurate GPCR homology models[5,6]. Due to the lack of structural conservation in the second extracellular loop, only a segment of seven residues, including the conserved Cys that connects this loop with TM3 via a disulfide bridge and the six following residues, was modeled for this domain. Most of the third intracellular loop was also not included in our M3R model because this domain was not solved in the 2VT4 structure. The homology model of $G\alpha_q$ (residues 11- 350) was constructed on the basis of the structure of $G\alpha_{i1}$ in complex with $\beta_1\gamma_2$ in the presence of GDP (1GP2)[7], with which it shares 51.5% identity at the amino acid level. Since we wanted to build a model of the receptor-G protein complex in the inactive conformation, we used the structure of $G\alpha_i$ rather than one of the available $G\alpha_q$ crystal structures (2BCJ and 2RGN)[8,9] as a template (note that the published $G\alpha_q$ structures represent active $G\alpha_q$ conformations in complex with $GDP{\cdot}AlF_4^-$). However, the coordinates of the C-terminal $G\alpha_q$ residues (351-358) were taken directly from the 2RGN $G\alpha_q$ crystal structure, since the corresponding residues of $G\alpha_{i1}$ were not solved in 1GP2. Note that the last residue of $G\alpha_q$, V359, was not included in our model because it was not solved in the 2RGN structure[9]. The coordinates of the $\beta_1\gamma_2$ complex were obtained from the 1GP2 structure[7].

Docking of the G protein heterotrimer to the M3R. The initial model of the M3R/G_q docked complex was manually formed in the Maestro user interface of the Schrödinger package. Following their construction, the docking partners were assembled guided by the cross-linking data. In particular, we tried to keep the distances between Cα atoms of pairs of receptor/G protein residues involved in agonist-independent cross-linking below the threshold of 15 Å, the maximum distance between the Cα atoms of two Cys residues that may still allow disulfide bridge formation due to conformational flexibility of the two proteins (see **Supplementary Table 3**). This was achieved by placing the N-terminus of $G\alpha_q$ in proximity of the i2 loop of the M3R, and pointing the C-terminal α helix of $G\alpha_q$ diagonally towards the intracellular opening of the M3R, between the i2 loop and H8. **Supplementary Table 3** indicates that it is not possible for the five C-

terminal residues of $G\alpha_q$ to be simultaneously located in close proximity of both the i2 loop and H8 of the M3R, indicative of a very high degree of conformational flexibility of the extreme C-terminus of $G\alpha_q$. As an additional guide for model building, we made sure that the N-terminus of $G\alpha_q$ and the C-terminus of Gγ, both of which are anchored to the plasma membrane through lipid modifications, were in proximity of the putative plane of the membrane. This manually assembled complex was then subjected to a perturbation docking run, as implemented in the RosettaDock functionality of Rosetta++ version 2.3 (refs. 10, 11). Given that the N-terminus of $G\alpha_q$, unlike the C-terminus, cross-links with only one specific region of the M3R, *i.e*. the i2 loop, we used the distance between the Cα atoms of R31 of $G\alpha_q$ and L173 of M3R as the sole constraint for the perturbation run. This distance was set at a maximum of 17 Å in order to obtain a large number of docking complexes, from which to choose the final model. The input complex was subjected to a full prepacking, in which the components were separated, repacked separately, and put back together, with off-rotamer sampling of side chains and extra conformations (nine rotamers) for chi1 and chi2 angles added in side-chain packing. The perturbation allowed off-rotamer side-chain modeling during the Monte-Carlo full atom minimization docking run. The M3R was initially normally perturbed by 3 Å along the line of centers and by 8 Å in the plane perpendicular to the line of centers, and rotated by 8° along the line of centers. Using this procedure, 2500 decoys were generated, scored, and ranked. The Cα distances between all residues identified in the cross-linking experiments were calculated for all output decoys, leading to the selection of the model most consistent with the observed cross-linking data (**Supplementary Table 3;** also see **Fig. 6** and text for details**)**.

Supplementary Results

Mass spectrometry experiments confirm the identity of a representative $G\alpha_q$/M3R complex

We carried out LC/MS/MS studies to obtain partial sequence information to authenticate the identity of the ~80 kDa immunoreactive band observed in the cross-linking studies.

Specifically, we obtained a representative $G\alpha_q$/M3R complex (N357C-$G\alpha_q$/T556C-M3R) via co-immunoprecipitation with the polyclonal anti-M3R antibody**,** excised the ~80 kDa immunoreactive band seen on Western blots (**Fig. 3b,** right panel), and then subjected this band to in-gel trypsin digestion and nanospray ESI LC/MS/MS (tandem mass spectroscopy). The MS/MS spectra were assigned to specific peptide sequences by using the Mascot (Matrix Sciences, London, UK) search algorithm or by manual inspection. The Mascot score for N357C-$G\alpha_q$ was excellent (671; generally, a Mascot score >60 is considered a reliable indicator of proper protein identification). Overall, 14 unique tryptic peptides could be assigned to N357C-$G\alpha_q$ with a score >30 (the protein sequence coverage was 51%). One of the peptides (Mascot score: 77; sequence: SLWNDPGIQEAYDR) contained the C144A point mutation that is specific for the engineered $G\alpha_q$ subunits used in the present study. Since this peptide sequence is not found in any naturally occurring protein, the identification of this peptide alone is sufficient to confirm the presence of the modified $G\alpha_q$ subunit (see **Supplementary Fig. 6a** for a representative MS/MS spectrum and the corresponding sequence assignment).

The presence of the T556C-M3R protein in the excised ~80 kDa band was confirmed by manual sequence assignment of the MS/MS spectrum shown in **Supplementary Fig. 6b** to the following M3R-derived tryptic peptide sequence: ELAGLQASGTEIEGR. This sequence is not present in any naturally occurring protein but is specific for the modified M3Rs used in this study (the identified M3R peptide corresponds to a portion of the modified i3 loop). Taken together, these data provide compelling evidence that the ~80 kDa immunoreactive species observed in the cross-linking experiments do indeed represent $G\alpha_q$/M3R complexes.

References

1. Chen, J.-G., Liu-Chen, S. & Rudnick, G. External cysteine residues in the serotonin transporter. *Biochemistry* **36**, 1479-1486 (1997).

2. Labute, P. Protonate3D: assignment of ionization states and hydrogen coordinates to macromolecular structures. *Proteins* **75**, 187-205 (2009).

3. Labute, P. The generalized Born/volume integral implicit solvent model: estimation of the free energy of hydration using London dispersion instead of atomic surface area. *J. Comput. Chem.* **29**, 1693-1698 (2008).

4. Warne, T. *et al*. Structure of a β_1-adrenergic G-protein-coupled receptor. *Nature* **454**, 486-491 (2008).

5. Costanzi, S. On the applicability of GPCR homology models to computer-aided drug discovery: a comparison between in silico and crystal structures of the β_2-adrenergic receptor. *J. Med. Chem.* **51**, 2907-2914 (2008).

6. Michino, M. *et al*. Community-wide assessment of GPCR structure modelling and ligand docking: GPCR Dock. *Nat. Rev. Drug. Discov.* **8**, 455-463 (2009).

7. Wall, M.A. *et al*. The structure of the G protein heterotrimer $G_i\alpha_1\beta_1\gamma_2$. *Cell* **83**, 1047-1058 (1995).

8. Tesmer, V.M., Kawano, T., Shankaranarayanan, A., Kozasa, T. & Tesmer, J.J. Snapshot of activated G proteins at the membrane: the $G\alpha_q$-GRK2-$G\beta\gamma$ complex. *Science* **310**, 1686-1690 (2005).

9. Lutz, S. *et al*. Structure of $G\alpha_q$-p63RhoGEF-RhoA complex reveals a pathway for the activation of RhoA by GPCRs. *Science* **318**, 1923-1927 (2007).

10. Gray, J.J. *et al.* Protein-protein docking with simultaneous optimization of rigid body displacement and side chain conformations. *J. Mol. Biol.* **331**, 281-299 (2003).

11. Wang, C. *et al.* Improved side-chain modeling for protein-protein docking. *Protein Sci.* **14**, 1328-1339 (2005).

Legends for supplementary figures

Supplementary Figure 1 Cross-linking of $G\alpha_q$ subunits containing C-terminal Cys substitutions with Cys-substituted mutant M3Rs. (**a-e**) Disulfide cross-linking studies with $G\alpha_q$ subunits containing the E355C (**a**), Y356C (**b**), N357C (**c**), L358C (**d**), or V359C (**e**) point mutations. Membranes prepared from COS-7 cells co-expressing the indicated mutant $G\alpha_q$ and M3R proteins were incubated with 100 μM Cu-Phen in the absence (-) or presence (+) of 1 mM carbachol (CCh). Western blots were probed with a monoclonal anti-$G\alpha_q$ antibody (non-reducing conditions). The blots shown are representative of two independent experiments. The bands corresponding to cross-linked receptor/$G\alpha_q$ complexes are indicated by arrows.

Supplementary Figure 2 Cross-linking experiments with $G\alpha_q$ subunits containing C-terminal Cys substitutions and Cys-substituted mutant M3Rs. (**a-e**) Disulfide cross-linking studies with $G\alpha_q$ subunits containing the E355C (**a**), Y356C (**b**), N357C (**c**), L358C (**d**), or V359C (**e**) point mutations. Membranes prepared from COS-7 cells co-expressing the indicated mutant $G\alpha_q$ and M3R proteins were incubated with 100 μM Cu-Phen in the absence (-) or presence (+) of 1 mM carbachol (CCh). All $G\alpha_q$ constructs could be cross-linked to the T556C mutant M3R (positive control). The cross-linked $G\alpha_q$/M3R-T556 complexes appear as ~80 kDa bands (arrows). Note that no cross-links could be detected between the five $G\alpha_q$ subunits and any of the other mutant M3Rs shown in this figure. The blots shown are representative of two independent experiments. Western blots were probed with a monoclonal anti-$G\alpha_q$ antibody (non-reducing conditions).

Supplementary Figure 3 Cross-linking analysis of representative $G\alpha_q$ subunits containing C-terminal Cys substitutions. **(a, b)** Cross-link formation between the L358C $G\alpha_q$ construct and the T556C M3R. Membranes from transfected COS-7 cells were incubated with either 100 μM Cu-Phen (**a**) or the Cys-specific, bifunctional cross-linker, BMOE (0.5 mM; (**b**)). Cross-linking experiments were performed in the absence (-) or presence (+) of 1 mM carbachol (CCh). Western blotting studies were carried out under

non-reducing (**a**) or reducing (**b**) conditions. (**c)** Effect of atropine and GTPγS treatment on the formation of the N357C-Gα_q/L176C-M3R complex. Cu-Phen (100 μM) was used to promote disulfide cross-link formation. Western blotting studies were carried out under non-reducing conditions, in the absence of carbachol. Note that GTPγS (100 μM) treatment greatly reduced the intensities of the observed cross-linking signals, while atropine (10 μM), an inverse muscarinic agonist, had no effect on the efficiency of the formation of the Gα_q/M3R complexes. The blots shown are representative of four independent experiments. The antibodies used are indicated underneath the blots. The immunoreactive bands corresponding to cross-linked receptor/Gα_q species are indicated by arrows.

Supplementary Figure 4 Cross-linking of Gα_q subunits containing C-terminal Cys substitutions with mutant M3Rs containing Cys substitutions within H8. (**a-c**) Disulfide cross-link formation between mutant Gα_q subunits containing C-terminal Cys substitutions and M3R-K548C (**a**), M3R-T549C (**b**), and M3R-T552C (**c**). Membranes prepared from COS-7 cells co-expressing the indicated mutant Gα_q and M3R proteins were incubated with 100 μM Cu-Phen in the absence (-) or presence (+) of 1 mM carbachol (CCh). Western blots were probed with a monoclonal anti-Gα_q antibody (non-reducing conditions). The blots shown are representative of two independent experiments. The bands corresponding to cross-linked receptor/Gα_q complexes are indicated by arrows.

Supplementary Figure 5 Co-immunoprecipitation experiments confirming the identity of selected Gα_q/M3R complexes. Co-immunoprecipitation were carried out with lysates prepared from COS-7 cells co-expressing the R31C-Gα_q/L173C-M3R (**a, b**) or the D321C-Gα_q/K548C-M3R (**c, d**) combinations. For control purposes, COS-7 cells were also transfected with the individual receptors or G protein subunits alone. To induce cross-link formation, membrane proteins prepared from transfected COS-7 cells were incubated with either 100 μM Cu-Phen (R31C-Gα_q/L173C-M3R) or 0.5 mM BMOE (D321C-Gα_q/K548C-M3R). Following membrane lysis, M3R-containing proteins were immunoprecipitated with a polyclonal anti-M3 antibody, followed by Western blotting

studies using an anti-$G\alpha_q$ monoclonal antibody **(a, c)**. In a reciprocal fashion, $G\alpha_q$-containing proteins were immunoprecipitated with the anti-$G\alpha_q$ antibody, followed by immunoblotting studies using the anti-M3R antibody **(b, d)**. Co-immunoprecipitation experiments were carried out as described under **Supplementary Methods**. The panels to the left show Western blots of samples prior to immunoprecipitation. In all co-immunoprecipitation experiments, the ~80 kDa band was the only immunoreactive species that was consistently detectable by both the anti-M3 and anti-$G\alpha_q$ antibodies. The co-immunoprecipitation studies also convincingly confirmed the agonist-dependence of cross-linking between the D321C-$G\alpha_q$ and the K548C-M3R proteins (**c, d)**. In this case, cross-linking experiments were carried out in the absence (-) or presence (+) of 1 mM carbachol (CCh). The blots shown are representative of two independent experiments. The bands corresponding to cross-linked receptor/$G\alpha_q$ complexes are indicated by arrows.

Supplementary Figure 6 Representative MS/MS spectra of the in-gel tryptic digest of the ~80 kDa band with manually assigned amino acid sequence information. We excised the ~80 kDa immunoreactive band corresponding to a representative $G\alpha_q$/M3R complex (N357C-$G\alpha_q$/T556C-M3R) from polyacrylamide gels (following co-immunoprecipitation of the $G\alpha_q$/M3R complex). (**a**) Manual assignment of the observed CID fragment ions to a tryptic $G\alpha_q$ peptide (SLWNDPGIQEAYDR). This peptide contains the C144A point mutation that is specific for the engineered $G\alpha_q$ subunits used in the present study and is not found in any naturally occurring protein. (**b**) Manual assignment of the observed CID fragment ions to a tryptic M3R peptide (ELAGLQASGTEIEGR). This peptide sequence is not present in any naturally occurring protein but is specific for the modified M3Rs used in this study (the identified M3R peptide corresponds to a portion of the modified i3 loop).

Supplementary Figure 7 Cross-linking experiments with $G\alpha_q$ subunits containing Cys substitutions within the N-terminal αN helix (G_q heterotrimer) and Cys-substituted mutant M3Rs. (**a-e**) Disulfide cross-linking studies with $G\alpha_q$ subunits containing the R19C (**a**), R20C (**b**), R27C (**c**), R30C (**d**), or R31C (**e**) point mutations. Membranes

prepared from COS-7 cells co-expressing the indicated mutant $G\alpha_q$ and M3R proteins were incubated with 100 μM Cu-Phen in the absence (-) or presence (+) of 1 mM carbachol (CCh). The $G\alpha_q$-N357C/M3R-T556C combination was included as a positive control. The cross-linked $G\alpha_q$-N357C/M3R-T556C complexes appear as ~80 kDa bands (arrows). Note that no cross-links could be detected between the five $G\alpha_q$ subunits and any of the mutant M3Rs shown in this figure. The blots shown are representative of two independent experiments. Western blots were probed with a monoclonal anti-$G\alpha_q$ antibody (**a**, **b**, and **e**) or a rabbit polyclonal anti-$G\alpha_q$ antibody directed against the C-terminus of $G\alpha_q$ (**c** and **d**) (non-reducing conditions).

Supplementary Figure 8 Cross-link formation between a Cys residue introduced into the αN helix of $G\alpha_q$ (R31C) and a Cys residue substituted into the i2 loop of the M3R (L173C). Membranes prepared from transfected COS-7 cells were incubated with 100 μM Cu-Phen in the absence (-) or presence (+) of 1 mM carbachol (CCh). As a control, we processed membranes prepared from cells co-expressing the N357C-$G\alpha_q$/L173C-M3R combination in parallel. Western blotting studies were carried out under non-reducing conditions. The antibodies used are indicated underneath the blots. The blots shown are representative of three independent experiments. The bands corresponding to cross-linked receptor/$G\alpha_q$ complexes are indicated by arrows.

Supplementary Figure 9 Cross-linking experiments with $G\alpha_q$ subunits containing Cys substitutions within the α4/β6 loop and Cys-substituted mutant M3Rs. (**a-c**) Disulfide cross-linking studies with $G\alpha_q$ subunits containing the P318C (**a**), S320C (**b**), or D321C (**c**) point mutations. Membranes prepared from COS-7 cells co-expressing the indicated mutant $G\alpha_q$ and M3R proteins were incubated with 100 μM Cu-Phen in the absence (-) or presence (+) of 1 mM carbachol (CCh). The $G\alpha_q$-N357C/M3R-T556C combination was included as a positive control. The cross-linked $G\alpha_q$-N357C/M3R-T556C complexes appear as ~80 kDa bands (indicated by arrows). Note that no cross-links could be detected between the three $G\alpha_q$ subunits and any of the mutant M3Rs shown in this figure. The blots shown are representative of two independent experiments. Western blots were probed with a monoclonal anti-$G\alpha_q$ antibody (non-reducing conditions).

Supplementary Figure 10 Cross-linking experiments with $G\alpha_q$ subunits containing Cys substitutions within the α4/β6 loop and Cys-substituted mutant M3Rs. (**a-c**) Disulfide cross-linking studies with $G\alpha_q$ subunits containing the P318C (**a**), S320C (**b**), or D321C (**c**) point mutations. Membranes prepared from COS-7 cells co-expressing the indicated mutant $G\alpha_q$ and M3R proteins were incubated with the Cys-specific, bifunctional cross-linker, BMOE (0.5 mM), in the absence (-) or presence (+) of 1 mM carbachol (CCh). The $G\alpha_q$-N357C/M3R-T556C combination was included as a positive control. The cross-linked $G\alpha_q$-N357C/M3R-T556C complexes appear as ~80 kDa bands (arrows). Note that no cross-links could be detected between the three $G\alpha_q$ subunits and any of the mutant M3Rs shown in this figure. The blots shown are representative of two independent experiments. Western blots were probed with a monoclonal anti-$G\alpha_q$ antibody (reducing conditions).

Supplementary Figure 11 Cross-linked M3R/$G\alpha_q$ complexes are present on the cell surface. (**a**) Cross-linking of cell surface T556C M3Rs with the N357C $G\alpha_q$ subunit. (**b**) Cross-linking of cell surface K548C M3Rs with the D321C $G\alpha_q$ subunit. COS-7 cells were transfected with the indicated mutant $G\alpha_q$ and M3R constructs. Cell surface proteins were biotinylated as described under **Supplementary Methods**. Membrane proteins were then solubilized and treated with the BMOE (0.5 mM) cross-linking reagent. Biotinylated proteins were then isolated using streptavidin conjugated to agarose beads, followed by the release of bound proteins via incubation with Laemmli buffer containing 10% β-mercaptoethanol. The blots shown are representative of three independent experiments. Western blots were probed with a monoclonal anti-$G\alpha_q$ antibody (reducing conditions). The ~80 kDa bands correspond to cross-linked receptor/$G\alpha_q$ complexes (arrows).

Supplementary Figure 12 Lack of effect of reduced receptor densities on $G\alpha_q$/M3R cross-linking patterns. Cross-linking studies were carried out with membranes prepared from COS-7 cells co-expressing the following representative receptor/G protein combinations: (**a**) N357C-$G\alpha_q$/T556C-M3R and R31C-$G\alpha_q$/L173C-M3R, and (**b**) D321C-$G\alpha_q$/K548C-M3R. For control purposes, COS-7 cells were also transfected with

individual receptors or G protein subunits alone (**a**). In the co-expression experiments, we drastically reduced M3R expression levels to ~1 pmol/mg by reducing the amount of transfected receptor DNA (see Methods for details). To induce cross-link formation, membrane proteins prepared from transfected COS-7 cells were incubated with either 100 μM Cu-Phen (**a**) or 0.5 mM BMOE (**b**). Cross-linking experiments were carried out in the absence (-) or presence (+) of 1 mM carbachol (CCh). Western blots were probed with a polyclonal anti-M3 antibody ((**a**), non-reducing conditions; (**b**), reducing conditions). Panel (**b**) also depicts a blot obtained after prolonged exposure of the film to visualize the monomeric form of the receptor. The blots shown are representative of two independent experiments. The bands corresponding to cross-linked receptor/$G\alpha_q$ complexes are indicated by arrows.

Supplementary Figure 13 Alignment of the sequences of rat $G\alpha_{i1}$ (PDB ID: 1GP2), mouse $G\alpha_q$ (PDB ID: 2RGN), and human $G\alpha_q$. The bars above the sequences indicate secondary structures found in the crystal structures (red, α-helix; yellow, β-strand; blue, 1-4 turn; green, 1-5 turn).

Supplementary Figure 14 Alignment of the sequences of the turkey β_1-adrenergic receptor (PDB ID: 2VT4) and the rat M3R. The bars above the sequences indicate secondary structures found in the crystal structure of the β_1-adrenergic receptor (red, α-helix; blue, 1-4 turn; green, 1-5 turn).

SI Table 1: Ligand binding and functional properties of Cys-substituted mutant M_3 muscarinic receptors

COS-7 cells were transiently transfected with the indicated M3' (3C)-Xa-derived Cys-substituted mutant M_3 receptor constructs. Radioligand binding studies and PI assays were carried out as detailed under 'Methods'. Basal inositol monophosphate (IP) levels were 2,610 ± 43 (=100%) for the M3' (3C)-Xa construct. Data are given as means ± S.E.M. from two to four independent experiments, each performed in duplicate.

		[^{3}H]-NMS binding		Carbachol binding	Carbachol-induced IP production		
Receptor		K_D	B_{max}	K_i	EC_{50}	E_{max}	Basal IP
	Amino acid location	*pM*	*pmol/mg protein*	*μM*	*nM*	*fold above basal*	*%*
M3' (3C)-Xa		362 ± 14	15.0 ± 1.0	32.6 ± 1.3	323 ± 47	19.1 ± 0.7	100
D164C	TM3/i2 junction	877 ± 17	1.4 ± 0.2	26.4 ± 12.5	1,781 ± 93	20.8 ± 1.4	83 ± 3
R165C	TM3/i2 junction	413 ± 5	14.1 ± 0.2	44.5 ± 1.9	12,240 ± 2,140	17.8 ± 2.9	92 ± 5
Y166C	TM3/i2 junction	163 ± 1	1.3 ± 0.2	2.5 ± 0.1	452 ± 107	21.0 ± 0.3	93 ± 7
S168C	TM3/i2 junction	342 ± 1	14.2 ± 0.2	37.0 ± 1.3	903 ± 77	20.7 ± 2.4	86 ± 10
R171C	i2 loop	265 ± 26	6.4 ± 0.4	18.6 ± 3.0	241 ± 72	22.2 ± 2.2	100 ± 6
L173C	i2 loop	263 ± 19	7.9 ± 0.6	22.0 ± 0.6	1,575 ± 80	9.9 ± 1.8	67 ± 2
R176C	i2 loop	338 ± 20	10.0 ± 0.5	17.6 ± 1.0	149 ± 14	12.2 ± 1.6	90 ± 6
R183C	i2/TM4 junction	239 ± 5	7.0 ± 0.4	21.0 ± 1.1	219 ± 20	11.5 ± 2.2	98 ± 6
Y254C	bottom of TM5	258 ± 64	5.4 ± 0.35	23.3 ± 2.4	2,605 ± 215	9.7 ± 1.7	74 ± 1
A488C	bottom of TM6	262 ± 11	7.2 ± 0.2	5.4 ± 0.2	61 ± 19	17.5 ± 7.7	164 ± 42
A489C	bottom of TM6	390 ± 12	16.4 ± 0.5	29.3 ± 1.9	715 ± 196	19.2 ± 2.2	75 ± 10
L492C	bottom of TM6	344 ± 6	10.8 ± 0.8	7.3 ± 0.6	86 ± 01	14.0 ± 2.4	152 ± 27
S493C	bottom of TM6	350 ± 6	13.5 ± 0.9	21.0 ± 0.6	238 ± 30	18.4 ± 4.0	89 ± 11
K548C	H8	251 ± 16	7.1 ± 0.2	12.5 ± 1.6	660 ± 148	21.2 ± 0.5	96 ± 5
T549C	H8	307 ± 7	10.5 ± 0.9	14.9 ± 2.4	609 ± 135	21.8 ± 3.6	78 ± 1
T552C	H8	249 ± 1	8.2 ± 0.6	15.9 ± 0.7	326 ± 29	12.8 ± 1.3	86 ± 1
T556C	H8	367 ± 14	14.3 ± 0.2	21.8 ± 2.1	237 ± 31	14.6 ± 3.2	101 ± 1
L559C	H8	332 ± 1	12.0 ± 0.7	38.3 ± 1.6	797 ± 103	14.9 ± 3.3	78 ± 8

SI Table 2: Functional properties of Cys-substituted mutant $G\alpha_q$ subunits

HEK-293 cells were co-transfected with expression plasmids coding for the porcine α_{2A}-adrenergic receptor and the indicated $G\alpha_q$ subunits. All Cys-substituted mutant $G\alpha_q$ subunits were derived from the $G\alpha_q$ C-less construct. PI assays were performed and analyzed as described under 'Methods'. Basal inositol monophosphate (IP) levels were 1,689 ± 194 dpm (=100%) for the wild-type (WT) $G\alpha_q$ construct. Data are given as means ± S.E.M. from two to five independent experiments, each performed in duplicate.

G protein		UK14304-induced IP production		
	Amino acid location	EC_{50} *nM*	E_{max} *Fold above basal*	Basal IP *(%)*
Vector		--	1.3 ± 0.1	83 ± 8
WT $G\alpha_q$		117 ± 42	8.0 ± 1.1	100
$G\alpha_q$ C-less		125 ± 48	8.4 ± 0.6	112 ± 3
R19C	αN helix	103 ± 13	5.7 ± 1.2	100 ± 9
R20C	αN helix	107 ± 55	3.7 ± 0.6	82 ± 7
R27C	αN helix	122 ± 23	4.3 ± 0.2	107 ± 4
R30C	αN helix	22 ± 9	4.1 ± 0.8	103 ± 3
R31C	αN helix	135 ± 48	5.9 ± 1.3	120 ± 19
P318C	α4/β6 loop	52 ± 9	7.4 ± 1.0	128 ± 2
S320C	α4/β6 loop	90 ± 1	8.6 ± 0.4	107 ± 14
D321C	α4/β6 loop	214 ± 76	8.4 ± 1.9	97 ± 7
K322C	α4/β6 loop	87 ± 15	9.2 ± 1.7	103 ± 6
E355C	C-terminus	197 ± 60	4.9 ± 0.4	105 ± 8
Y356C	C-terminus	101 ± 30	8.6 ± 1.4	113 ± 7
N357C	C-terminus	42 ± 22	10.0 ± 1.5	91 ± 6
L358C	C-terminus	275 ± 65	5.0 ± 0.3	89 ± 5
V359C	C-terminus	97 ± 33	9.7 ± 1.3	91 ± 10

SI Table 3: Distances between Cα atoms of pairs of M3R/$G\alpha_q$ residues involved in agonist-independent cross-linking

Domains $G\alpha_q$ - M3R	Residue Pairs $G\alpha_q$ - M3R	Distance between Cα atoms (Å)	
		Manually assembled model	Final model
N-term. - i2 loop	R31 - L173	14.28	13.32
C-term. - i2 loop	E355 - L173	14.85	16.42
	Y356 - L173	13.20	14.07
	N357 - L173	10.11	11.90
	L358 - L173	11.32	8.72
	E355 - R176	14.48	14.10
	Y356 - R176	11.65	10.91
	N357 - R176	9.24	8.99
C-term. - H8	E355 - T556	18.73	21.45
	Y356 - T549	8.39	13.12
	Y356 - T556	17.68	22.08
	N357 - T552	16.71	21.60
	N357 - T556	21.10	25.40
	L358 - T552	14.95	23.15
	L358 - T556	19.36	27.25

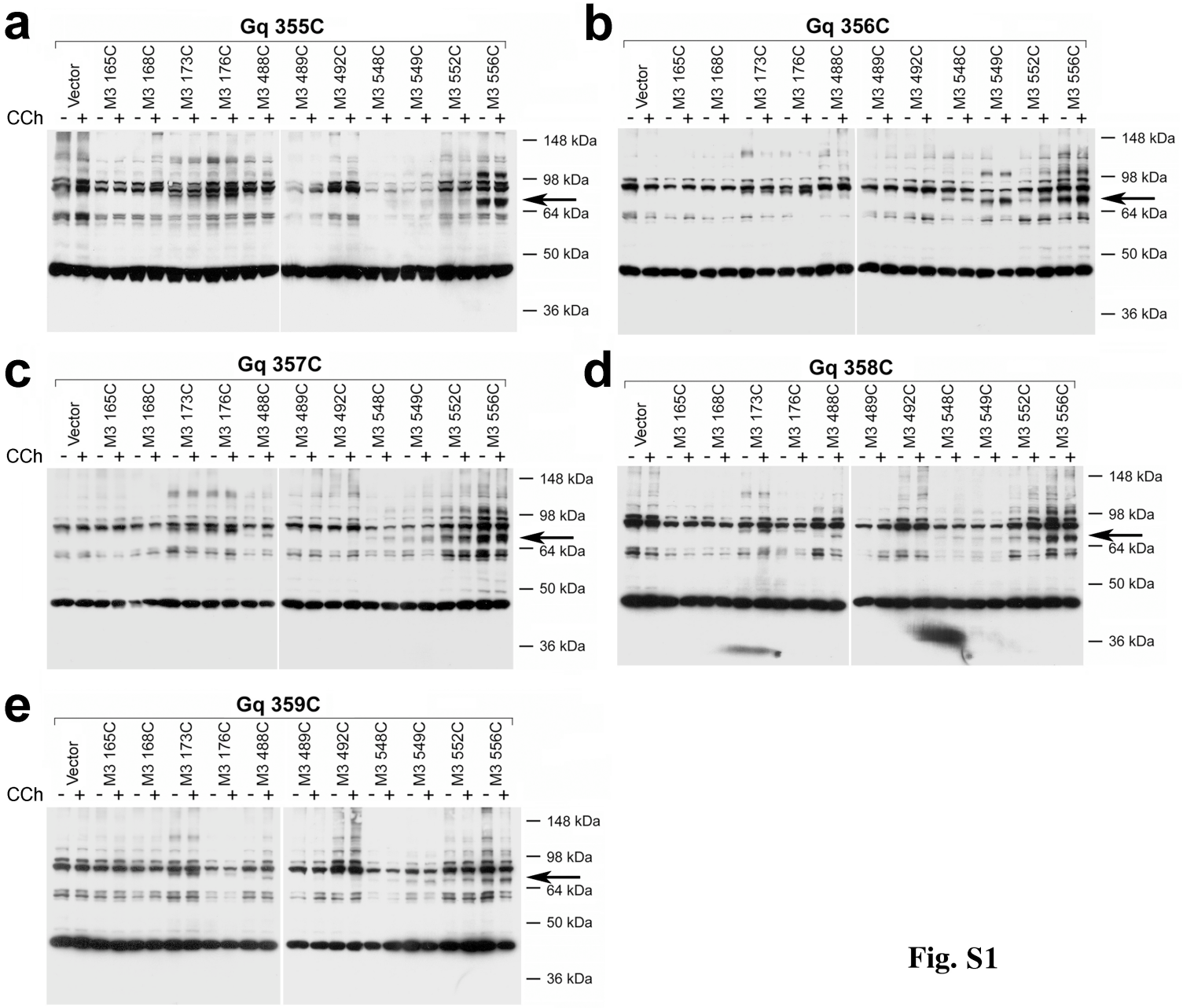
a
Gq 355C
b
Gq 356C
c
Gq 357C
d
Gq 358C
e
Gq 359C
Vector
M3 165C
M3 168C
M3 173C
M3 176C
M3 488C
M3 489C
M3 492C
M3 548C
M3 549C
M3 552C
M3 556C
CCh
148 kDa
98 kDa
64 kDa
50 kDa
36 kDa

Fig. S1

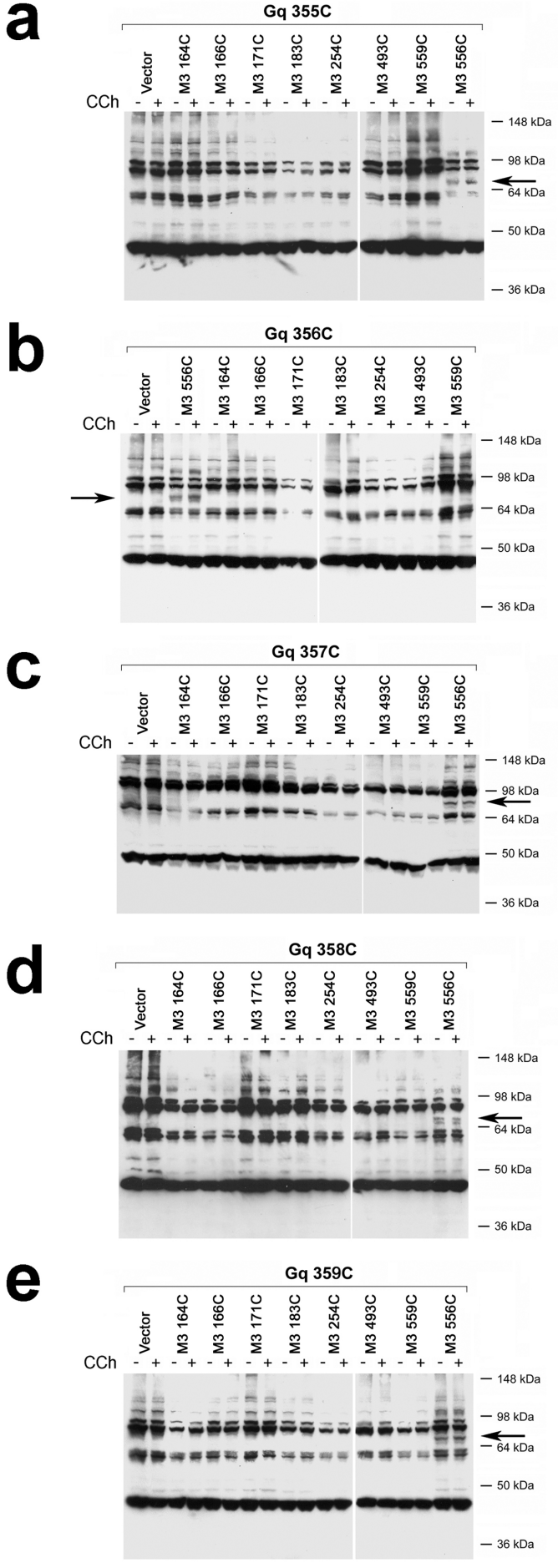
a
Gq 355C
Vector
M3 164C
M3 166C
M3 171C
M3 183C
M3 254C
M3 493C
M3 559C
M3 556C
CCh
148 kDa
98 kDa
64 kDa
50 kDa
36 kDa
b
Gq 356C
Vector
M3 556C
M3 164C
M3 166C
M3 171C
M3 183C
M3 254C
M3 493C
M3 559C
CCh
148 kDa
98 kDa
64 kDa
50 kDa
36 kDa
c
Gq 357C
Vector
M3 164C
M3 166C
M3 171C
M3 183C
M3 254C
M3 493C
M3 559C
M3 556C
CCh
148 kDa
98 kDa
64 kDa
50 kDa
36 kDa
d
Gq 358C
Vector
M3 164C
M3 166C
M3 171C
M3 183C
M3 254C
M3 493C
M3 559C
M3 556C
CCh
148 kDa
98 kDa
64 kDa
50 kDa
36 kDa
e
Gq 359C
Vector
M3 164C
M3 166C
M3 171C
M3 183C
M3 254C
M3 493C
M3 559C
M3 556C
CCh
148 kDa
98 kDa
64 kDa
50 kDa
36 kDa

Fig. S2

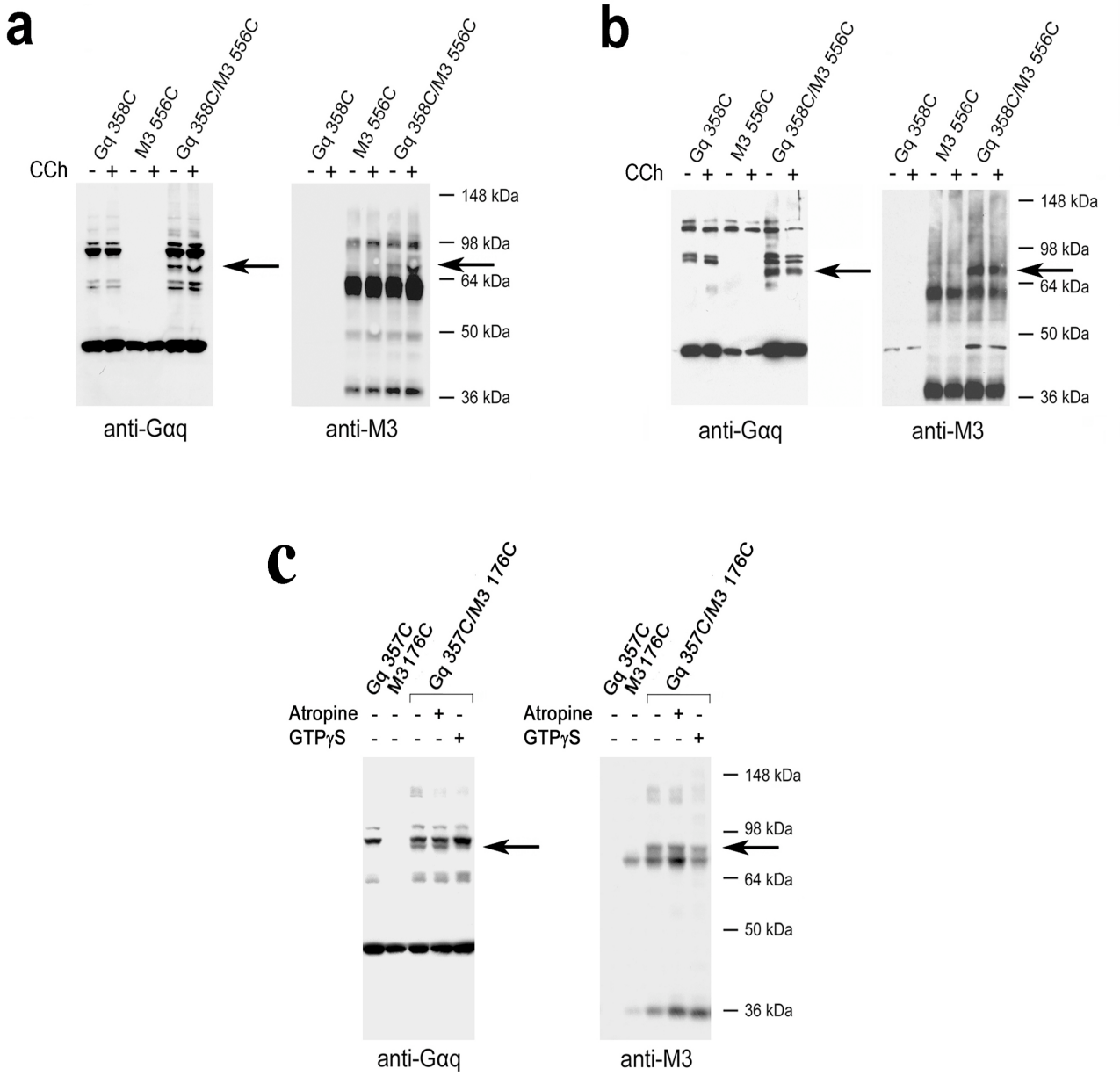
a
Gq 358C
M3 556C
Gq 358C/M3 556C
CCh
148 kDa
98 kDa
64 kDa
50 kDa
36 kDa
anti-Gαq
anti-M3
b
c
Gq 357C
M3 176C
Gq 357C/M3 176C
Atropine
GTPγS

Fig. S3

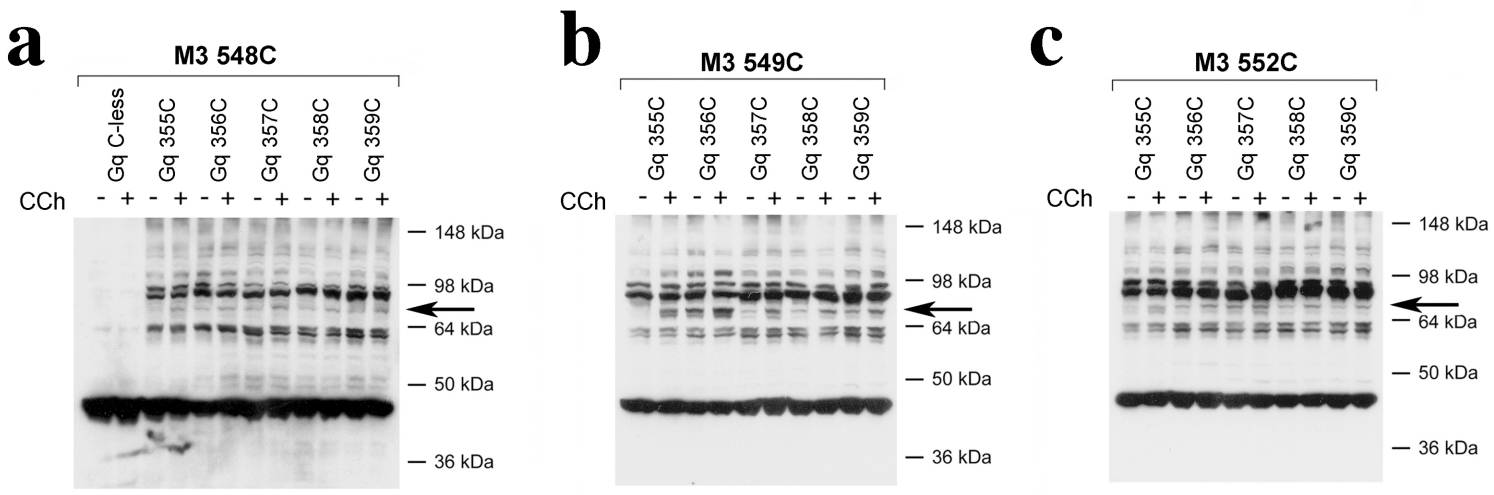
a
M3 548C
Gq C-less
Gq 355C
Gq 356C
Gq 357C
Gq 358C
Gq 359C
CCh
- + - + - + - + - + - +
148 kDa
98 kDa
64 kDa
50 kDa
36 kDa
b
M3 549C
Gq 355C
Gq 356C
Gq 357C
Gq 358C
Gq 359C
CCh
- + - + - + - + - +
148 kDa
98 kDa
64 kDa
50 kDa
36 kDa
c
M3 552C
Gq 355C
Gq 356C
Gq 357C
Gq 358C
Gq 359C
CCh
- + - + - + - + - +
148 kDa
98 kDa
64 kDa
50 kDa
36 kDa

Fig. S4

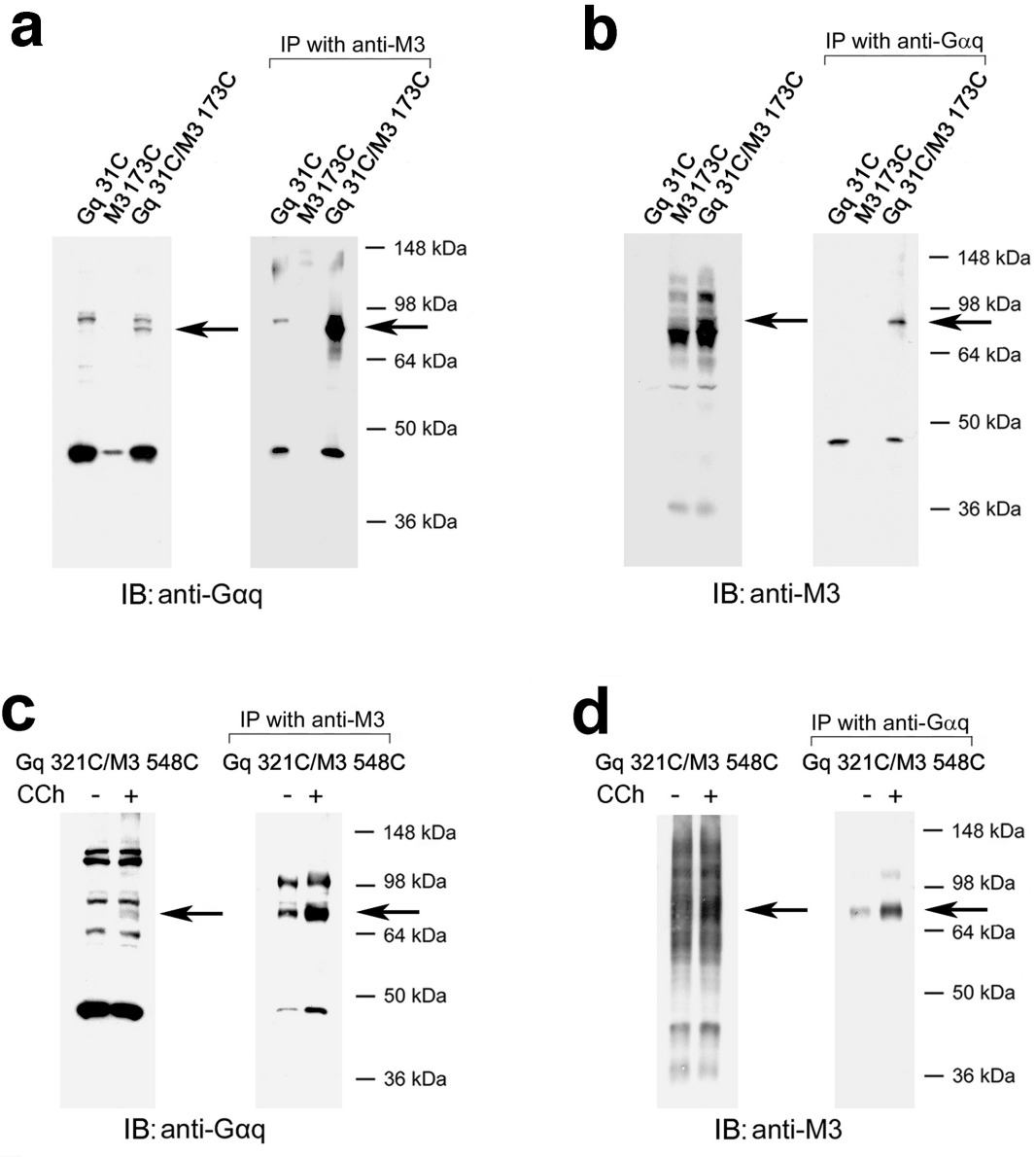
a
IP with anti-M3
Gq 31C
M3 173C
Gq 31C/M3 173C
Gq 31C
M3 173C
Gq 31C/M3 173C
148 kDa
98 kDa
64 kDa
50 kDa
36 kDa
IB: anti-Gαq
b
IP with anti-Gαq
Gq 31C
M3 173C
Gq 31C/M3 173C
Gq 31C
M3 173C
Gq 31C/M3 173C
148 kDa
98 kDa
64 kDa
50 kDa
36 kDa
IB: anti-M3
c
IP with anti-M3
Gq 321C/M3 548C
Gq 321C/M3 548C
CCh - +
- +
148 kDa
98 kDa
64 kDa
50 kDa
36 kDa
IB: anti-Gαq
d
IP with anti-Gαq
Gq 321C/M3 548C
Gq 321C/M3 548C
CCh - +
- +
148 kDa
98 kDa
64 kDa
50 kDa
36 kDa
IB: anti-M3

Fig. S5

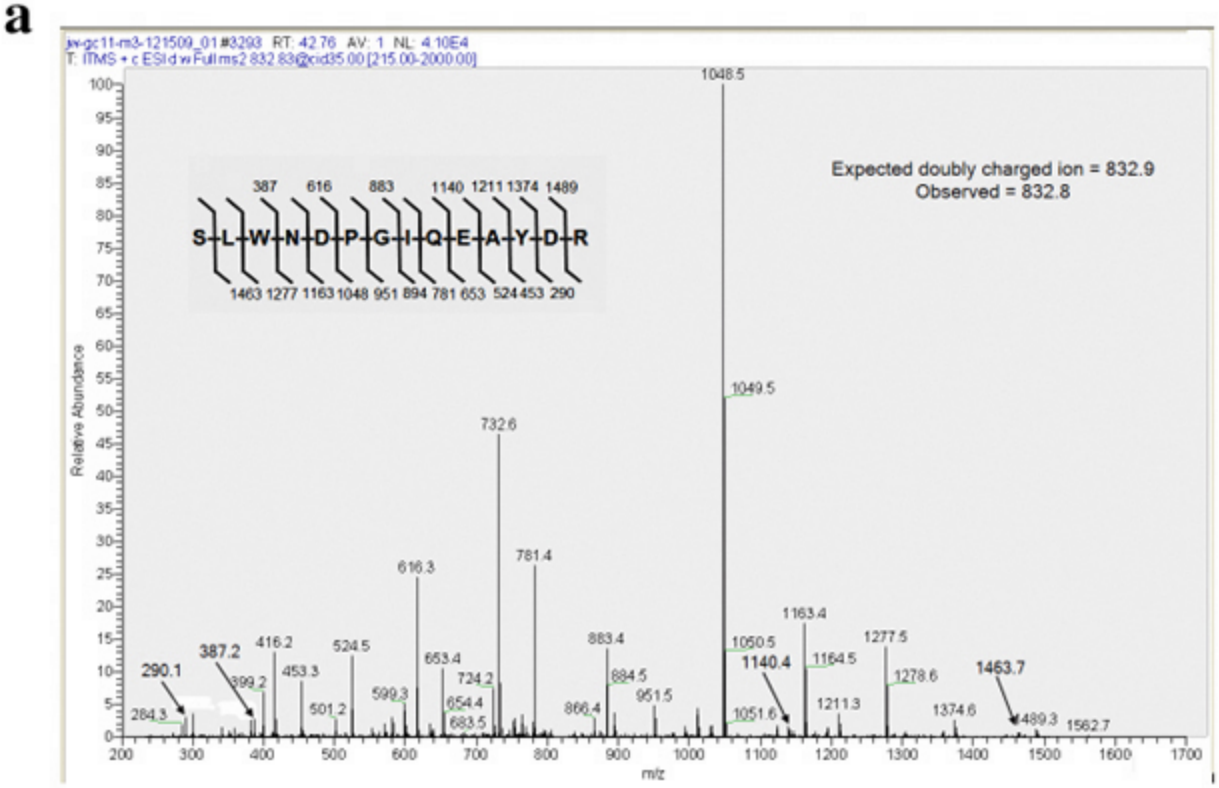
a
Expected doubly charged ion = 832.9
Observed = 832.8
S-L-W-N-D-P-G-I-Q-E-A-Y-D-R
387 616 883 1140 1211 1374 1489
1463 1277 1163 1048 951 894 781 653 524 453 290
Relative Abundance
m/z

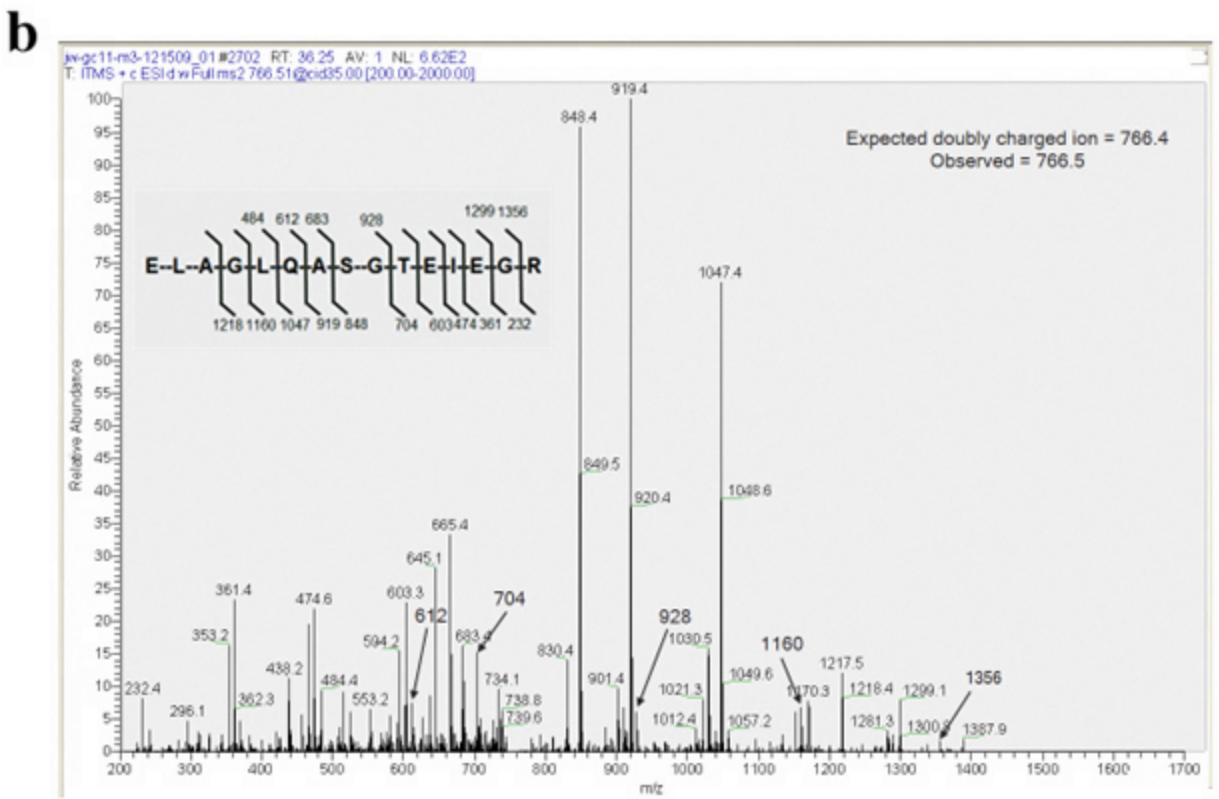
b
Expected doubly charged ion = 766.4
Observed = 766.5
E-L-A-G-L-Q-A-S-G-T-E-I-E-G-R
484 612 683 928 1299 1356
1218 1160 1047 919 848 704 603 474 361 232
Relative Abundance
m/z

Fig. S6

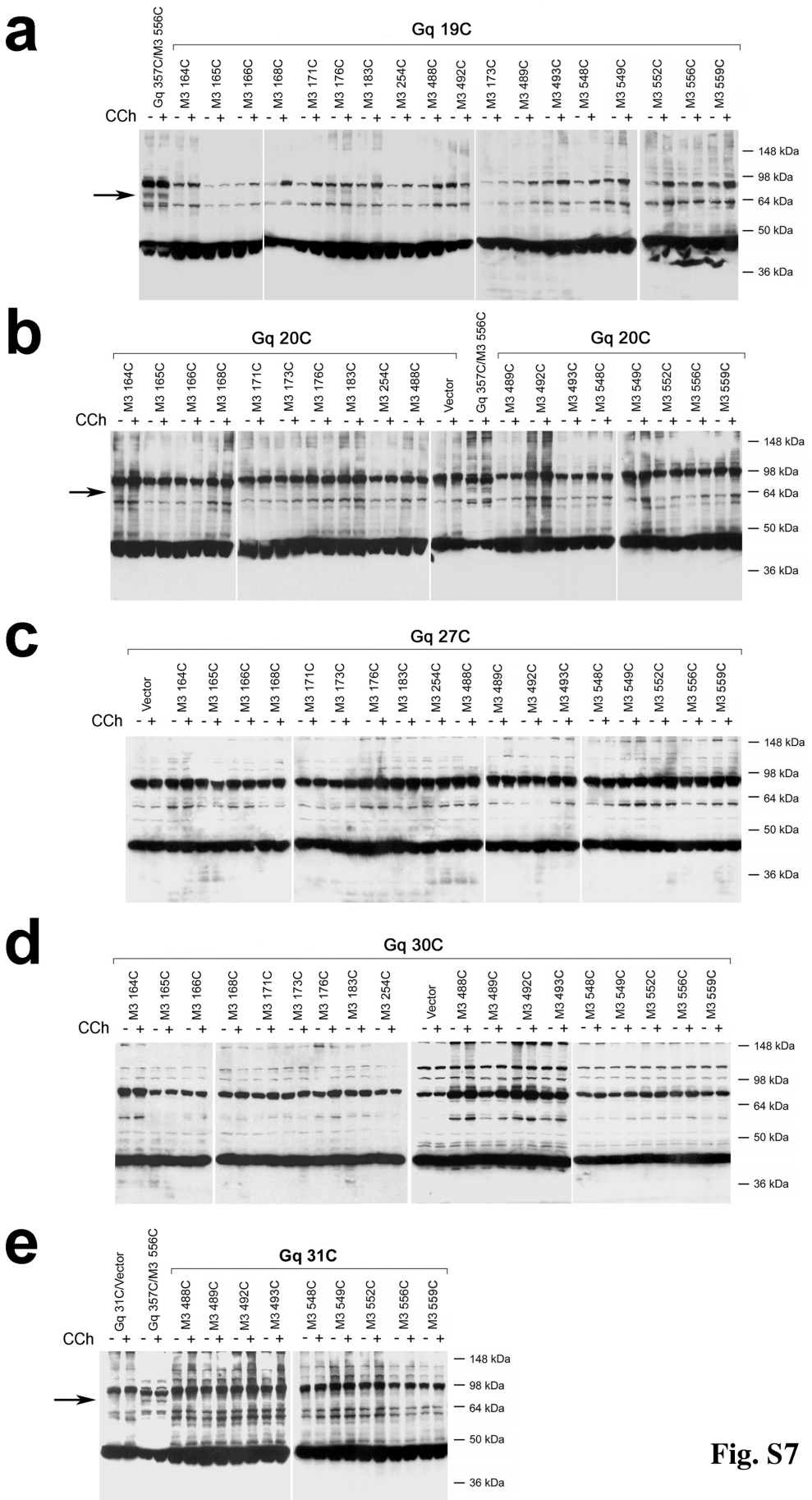
a
Gq 19C
Gq 357C/M3 556C
M3 164C
M3 165C
M3 166C
M3 168C
M3 171C
M3 176C
M3 183C
M3 254C
M3 488C
M3 492C
M3 173C
M3 489C
M3 493C
M3 548C
M3 549C
M3 552C
M3 556C
M3 559C
CCh
148 kDa
98 kDa
64 kDa
50 kDa
36 kDa
b
Gq 20C
Gq 357C/M3 556C
Gq 20C
M3 164C
M3 165C
M3 166C
M3 168C
M3 171C
M3 173C
M3 176C
M3 183C
M3 254C
M3 488C
Vector
M3 489C
M3 492C
M3 493C
M3 548C
M3 549C
M3 552C
M3 556C
M3 559C
CCh
148 kDa
98 kDa
64 kDa
50 kDa
36 kDa
c
Gq 27C
Vector
M3 164C
M3 165C
M3 166C
M3 168C
M3 171C
M3 173C
M3 176C
M3 183C
M3 254C
M3 488C
M3 489C
M3 492C
M3 493C
M3 548C
M3 549C
M3 552C
M3 556C
M3 559C
CCh
148 kDa
98 kDa
64 kDa
50 kDa
36 kDa
d
Gq 30C
M3 164C
M3 165C
M3 166C
M3 168C
M3 171C
M3 173C
M3 176C
M3 183C
M3 254C
Vector
M3 488C
M3 489C
M3 492C
M3 493C
M3 548C
M3 549C
M3 552C
M3 556C
M3 559C
CCh
148 kDa
98 kDa
64 kDa
50 kDa
36 kDa
e
Gq 31C
Gq 31C/Vector
Gq 357C/M3 556C
M3 488C
M3 489C
M3 492C
M3 493C
M3 548C
M3 549C
M3 552C
M3 556C
M3 559C
CCh
148 kDa
98 kDa
64 kDa
50 kDa
36 kDa

Fig. S7

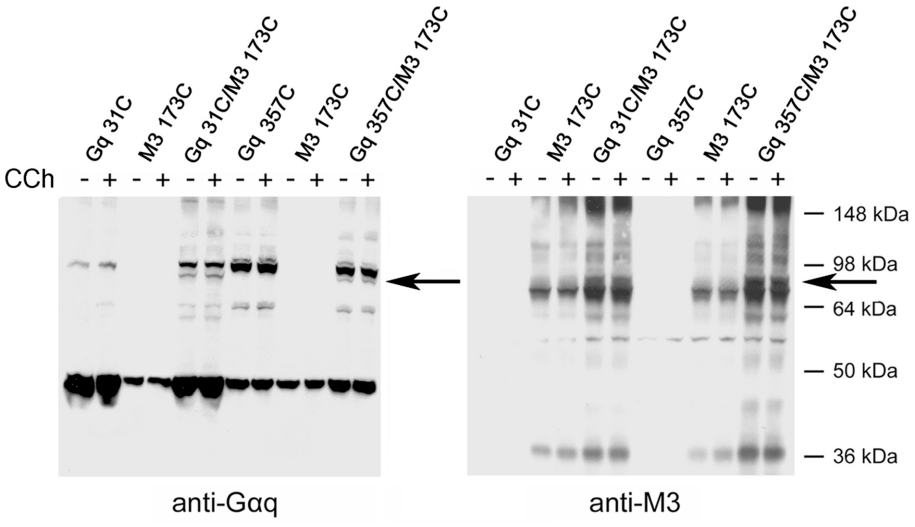
Gq 31C
M3 173C
Gq 31C/M3 173C
Gq 357C
M3 173C
Gq 357C/M3 173C
CCh
- + - + - + - + - + - +
anti-Gαq
Gq 31C
M3 173C
Gq 31C/M3 173C
Gq 357C
M3 173C
Gq 357C/M3 173C
- + - + - + - + - + - +
148 kDa
98 kDa
64 kDa
50 kDa
36 kDa
anti-M3

Fig. S8

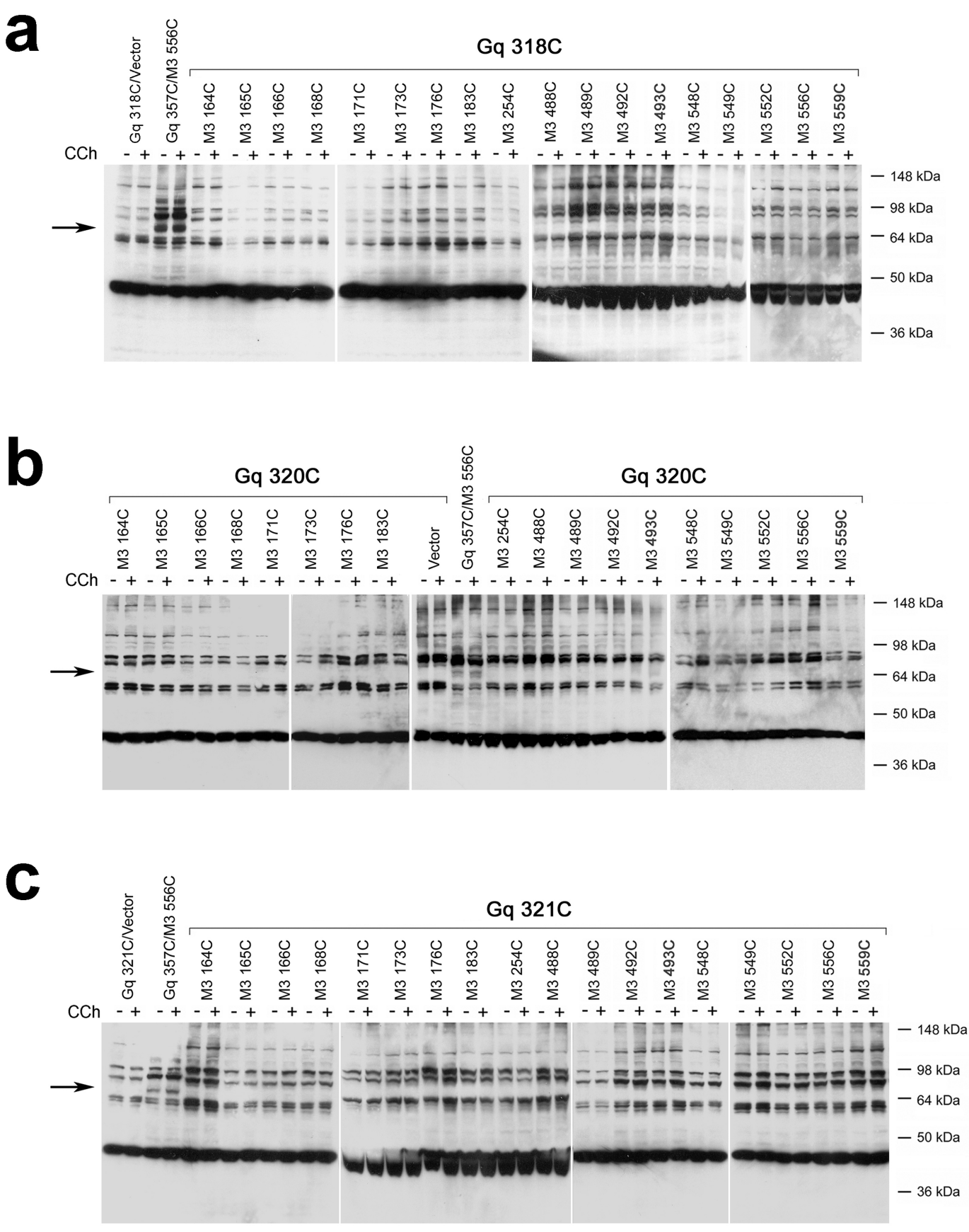
a
Gq 318C
Gq 318C/Vector
Gq 357C/M3 556C
M3 164C
M3 165C
M3 166C
M3 168C
M3 171C
M3 173C
M3 176C
M3 183C
M3 254C
M3 488C
M3 489C
M3 492C
M3 493C
M3 548C
M3 549C
M3 552C
M3 556C
M3 559C
CCh
148 kDa
98 kDa
64 kDa
50 kDa
36 kDa
b
Gq 320C
Gq 320C
Vector
Gq 357C/M3 556C
c
Gq 321C
Gq 321C/Vector

Fig. S9

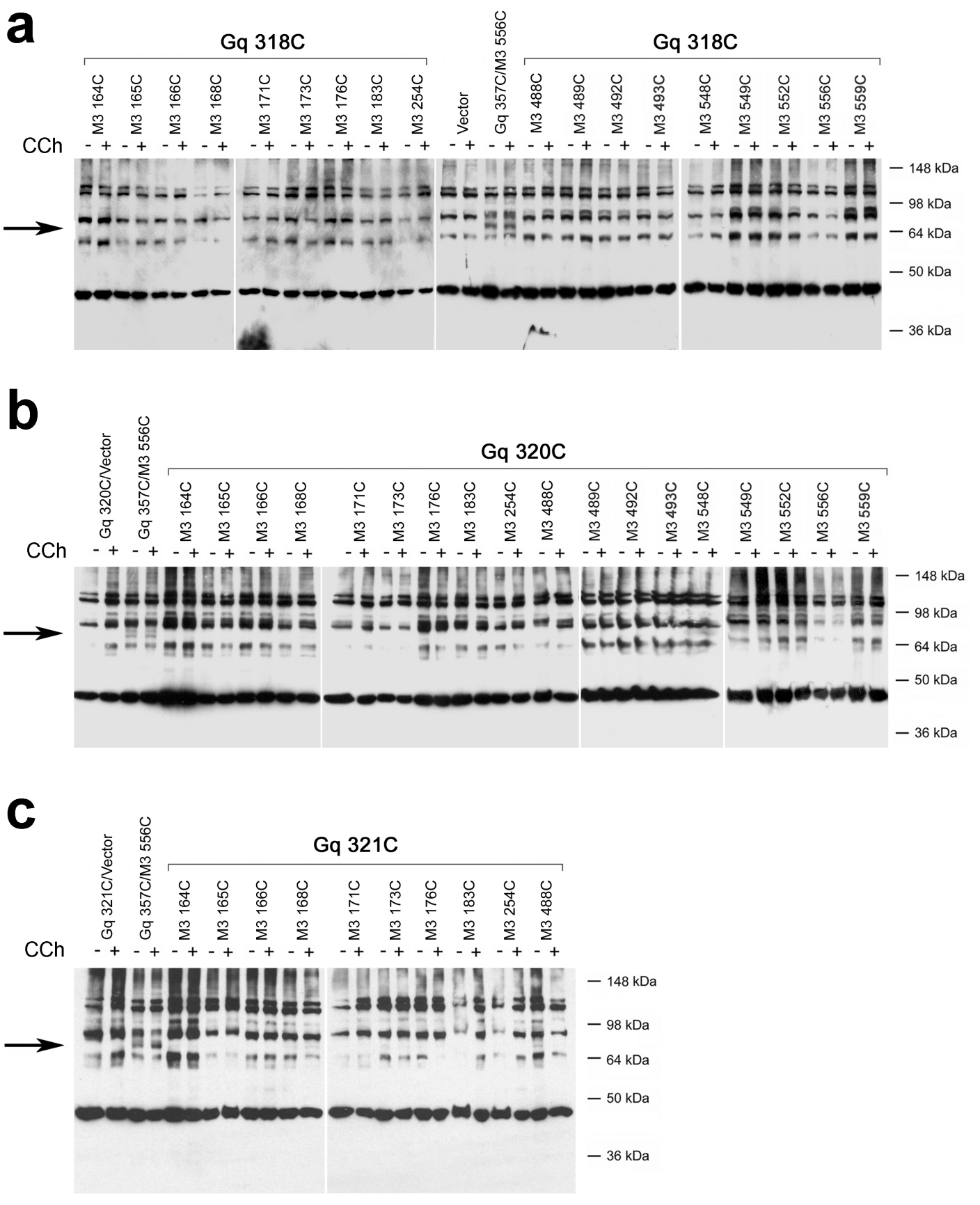
a
Gq 318C
Gq 318C
M3 164C
M3 165C
M3 166C
M3 168C
M3 171C
M3 173C
M3 176C
M3 183C
M3 254C
Vector
Gq 357C/M3 556C
M3 488C
M3 489C
M3 492C
M3 493C
M3 548C
M3 549C
M3 552C
M3 556C
M3 559C
CCh
148 kDa
98 kDa
64 kDa
50 kDa
36 kDa
b
Gq 320C/Vector
Gq 357C/M3 556C
Gq 320C
M3 164C
M3 165C
M3 166C
M3 168C
M3 171C
M3 173C
M3 176C
M3 183C
M3 254C
M3 488C
M3 489C
M3 492C
M3 493C
M3 548C
M3 549C
M3 552C
M3 556C
M3 559C
CCh
148 kDa
98 kDa
64 kDa
50 kDa
36 kDa
c
Gq 321C/Vector
Gq 357C/M3 556C
Gq 321C
M3 164C
M3 165C
M3 166C
M3 168C
M3 171C
M3 173C
M3 176C
M3 183C
M3 254C
M3 488C
CCh
148 kDa
98 kDa
64 kDa
50 kDa
36 kDa

Fig. S10

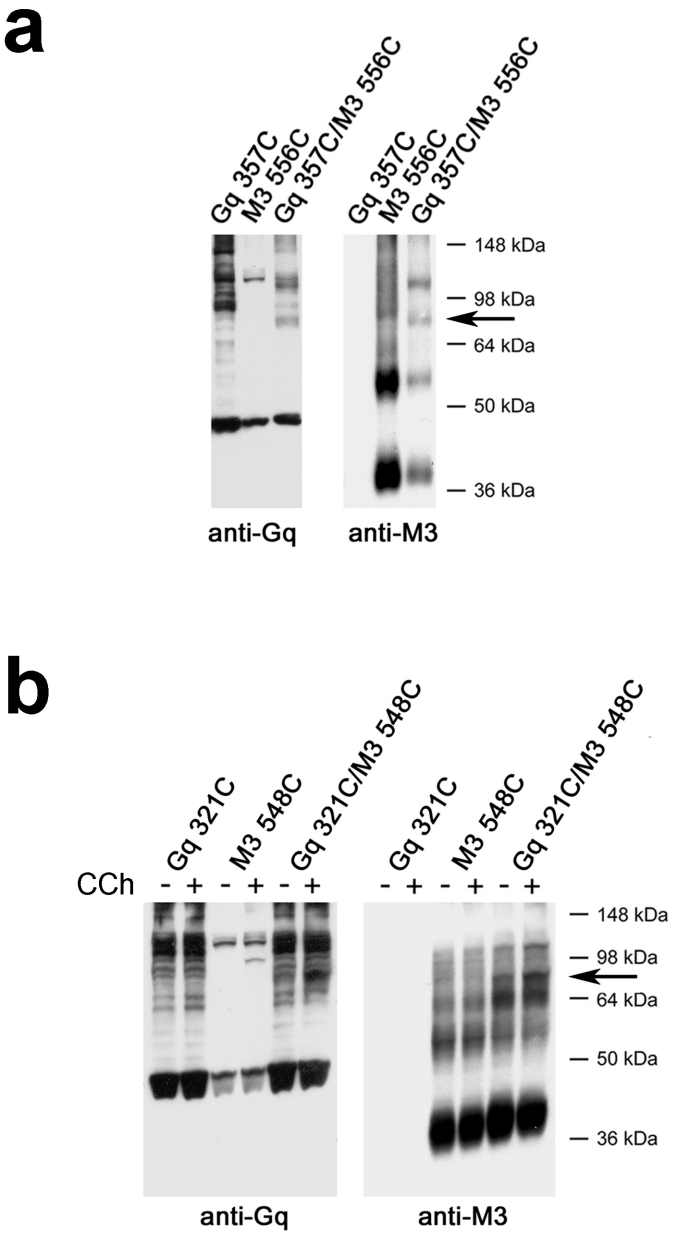
a
Gq 357C
M3 556C
Gq 357C/M3 556C
Gq 357C
M3 556C
Gq 357C/M3 556C
148 kDa
98 kDa
64 kDa
50 kDa
36 kDa
anti-Gq
anti-M3
b
Gq 321C
M3 548C
Gq 321C/M3 548C
Gq 321C
M3 548C
Gq 321C/M3 548C
CCh
- + - + - +
- + - + - +
148 kDa
98 kDa
64 kDa
50 kDa
36 kDa
anti-Gq
anti-M3

Fig. S11

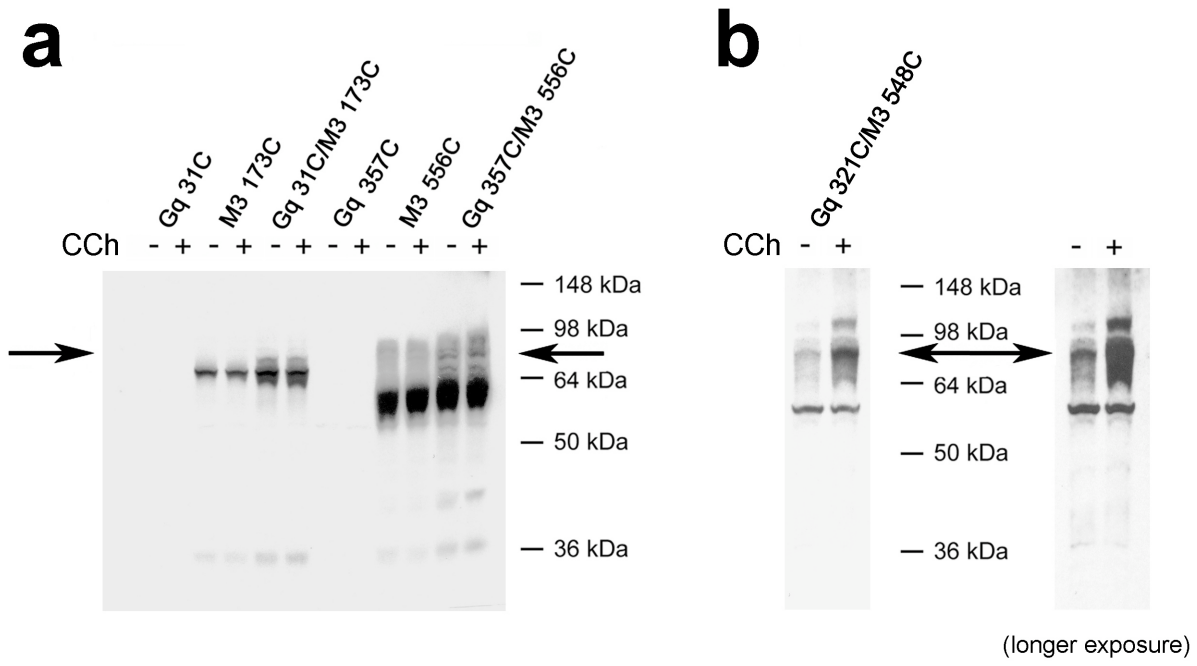
a
Gq 31C
M3 173C
Gq 31C/M3 173C
Gq 357C
M3 556C
Gq 357C/M3 556C
CCh - + - + - + - + - + - +
148 kDa
98 kDa
64 kDa
50 kDa
36 kDa
b
Gq 321C/M3 548C
CCh - +
- +
148 kDa
98 kDa
64 kDa
50 kDa
36 kDa
(longer exposure)

Fig. S12

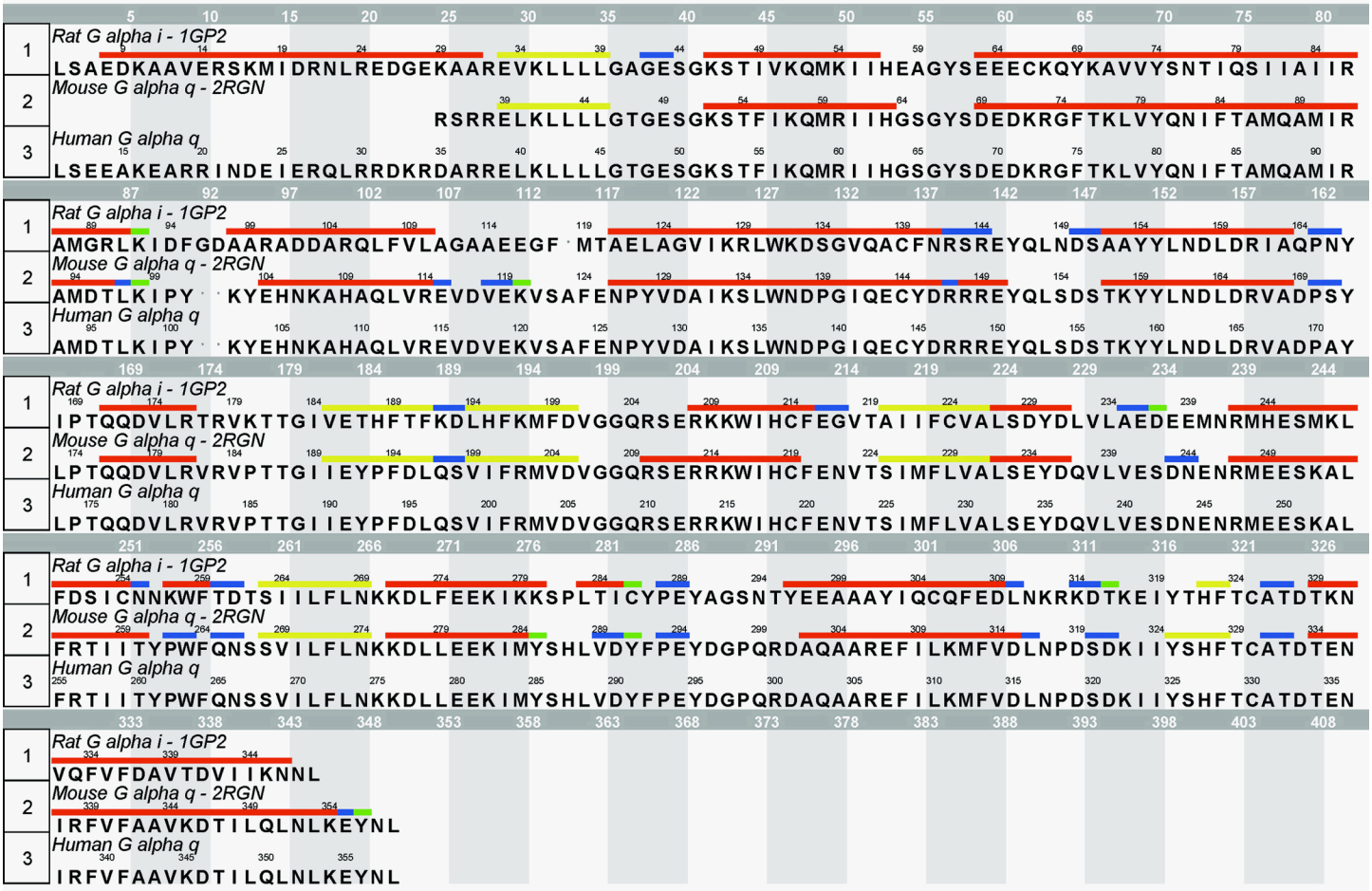
Rat G alpha i - 1GP2
LSAEDKAAVERSKMIDRNLREDGEKAAREVKLLLLGAGESGKSTIVKQMKIIHEAGYSEEECKQYKAVVYSNTIQSIIAIIR
Mouse G alpha q - 2RGN
RSRRELKLLLLGTGESGKSTFIKQMRIIHGSGYSDEDKRGFTKLVYQNIFTAMQAMIR
Human G alpha q
LSEEAKEARRINDEIERQLRRDKRDARRELKLLLLGTGESGKSTFIKQMRIIHGSGYSDEDKRGFTKLVYQNIFTAMQAMIR
Rat G alpha i - 1GP2
AMGRLKIDFGDAARADDARQLFVLAGAAEEGF MTAELAGVIKRLWKDSGVQACFNRSREYQLNDSAAYYLNDLDRIAQPNY
Mouse G alpha q - 2RGN
AMDTLKIPY KYEHNKAHAQLVREVDVEKVSAFENPYVDAIKSLWNDPGIQECYDRRREYQLSDSTKYYLNDLDRVADPSY
Human G alpha q
AMDTLKIPY KYEHNKAHAQLVREVDVEKVSAFENPYVDAIKSLWNDPGIQECYDRRREYQLSDSTKYYLNDLDRVADPAY
Rat G alpha i - 1GP2
IPTQQDVLRTRVKTTGIVETHFTFKDLHFKMFDVGGQRSERKKWIHCFEGVTAIIFCVALSDYDLVLAEDEEMNRMHESMKL
Mouse G alpha q - 2RGN
LPTQQDVLRVRVPTTGIIEYPFDLQSVIFRMVDVGGQRSERRKWIHCFENVTSIMFLVALSEYDQVLVESDNENRMEESKAL
Human G alpha q
LPTQQDVLRVRVPTTGIIEYPFDLQSVIFRMVDVGGQRSERRKWIHCFENVTSIMFLVALSEYDQVLVESDNENRMEESKAL
Rat G alpha i - 1GP2
FDSICNNKWFTDTSIILFLNKKDLFEEKIKKSPLTICYPEYAGSNTYEEAAAYIQCQFEDLNKRKDTKEIYTHFTCATDTKN
Mouse G alpha q - 2RGN
FRTIITYPWFQNSSVILFLNKKDLLEEKIMYSHLVDYFPEYDGPQRDAQAAREFILKMFVDLNPDSDKIIYSHFTCATDTEN
Human G alpha q
FRTIITYPWFQNSSVILFLNKKDLLEEKIMYSHLVDYFPEYDGPQRDAQAAREFILKMFVDLNPDSDKIIYSHFTCATDTEN
Rat G alpha i - 1GP2
VQFVFDAVTDVIIKNNL
Mouse G alpha q - 2RGN
IRFVFAAVKDTILQLNLKEYNL
Human G alpha q
IRFVFAAVKDTILQLNLKEYNL

Fig. S13

Fig. S 14